Circulation Journal
Official Journal of the Japanese Circulation Society
http://www.j-circ.or.jp

ORIGINAL ARTICLE
Arrhythmia/Electrophysiology

Chronic Amiodarone Therapy Impairs the Function of the Superior Sinoatrial Node in Patients With Atrial Fibrillation

Hee-Sun Mun, MD; Changyu Shen, PhD; Hui-Nam Pak, MD, PhD; Moon-Hyoung Lee, MD, PhD; Shien-Fong Lin, PhD; Peng-Sheng Chen, MD; Boyoung Joung, MD, PhD

Background: The mechanisms underlying amiodarone-induced sinoatrial node (SAN) dysfunction remain unclear, so we used 3-dimensional endocardial mapping of the right atrium (RA) to investigate.

Methods and Results: In a matched-cohort design, 18 patients taking amiodarone before atrial fibrillation (AF) ablation (amiodarone group) were matched for age, sex and type of AF with 18 patients who had undergone AF ablation without taking amiodarone (no-amiodarone group). The amiodarone group had a slower heart rate than the no-amiodarone group at baseline and during isoproterenol infusion. Only the amiodarone group had sick sinus syndrome (n=4, 22%, P=0.03) and abnormal (>550 ms) corrected SAN recovery time (n=5, 29%; P=0.02). The median distance from the junction of the superior vena cava (SVC) and RA to the most cranial earliest activation site (EAS) was longer in the amiodarone group than in the no-amiodarone group at baseline (20.5 vs. 10.6 mm, P=0.04) and during isoproterenol infusion (12.8 vs. 6.3 mm, P=0.03). The distance from the SVC-RA junction to the EAS negatively correlated with the P-wave amplitudes of leads II (r=–0.47), III (r=–0.60) and aV_F (r=–0.56) (P<0.001 for all).

Conclusions: In a quarter of the AF patients, amiodarone causes superior SAN dysfunction, which results in a downward shift of the EAS and reduced P-wave amplitude in leads II, III and aV_F at baseline and during isoproterenol infusion. (*Circ J* 2013; **77:** 2255–2263)

Key Words: Amiodarone; Atrial fibrillation; Sick sinus syndrome; Sympathetic nervous system

As the elderly population continues to expand, atrial fibrillation (AF) is becoming an increasingly common medical condition.[1–4] Amiodarone is the most frequently used agent for maintaining sinus rhythm in patients with AF, but it impairs sinoatrial node (SAN) function in a significant number of patients.[5] SAN automaticity is maintained by synergistic actions of a "voltage clock" mediated by voltage-sensitive membrane ionic currents such as the hyperpolarization-activated pacemaker current (I_f)[6] and a "Ca^{2+} clock" mediated by rhythmic spontaneous sarcoplasmic reticular (SR) Ca^{2+} release.[7] The Ca^{2+} clock of the superior SAN is primarily responsible for rate acceleration during sympathetic stimulation[8,9] and its unresponsiveness to sympathetic stimulation is a characteristic finding in dogs with AF and heart failure.[10,11] Because amiodarone has inhibitory effects on multiple channels (I_{to}, I_{Kr}, I_{Ks}, I_{Ca}, I_{Na}) because of its β-adrenergic blocking effect,[12] it might impair SAN function by suppressing the voltage and Ca^{2+} clocks. Using the 3-dimensional (3D) endocardial electroanatomical mapping techniques, we found that unresponsiveness of the superior SAN to sympathetic stimulation is a characteristic finding in patients with AF and symptomatic bradycardia.[13]

Editorial p2240

The purpose of the present study was to study the mechanisms of SAN dysfunction caused by amiodarone using the 3D mapping techniques. The results are used to test the hypothesis that unresponsiveness of the superior SAN to sympathetic stimulation (superior SAN dysfunction) underlies the mechanisms of SAN dysfunction in AF patients taking amiodarone.

Received December 28, 2012; revised manuscript received March 25, 2013; accepted April 18, 2013; released online June 4, 2013 Time for primary review: 24 days

Division of Cardiology, Department of Medicine, Yonsei University College of Medicine, Seoul (H.-S.M., H.-N.P., M.-H.L., B.J.); Division of Cardiology, Department of Internal Medicine, Kangnam Sacred Heart Hospital, Hallym University Medical Center, Seoul (H.-S.M.), Korea; and the Department of Biostatistics (C.S.), the Krannert Institute of Cardiology (S.-F.L., P.-S.C.), the Division of Cardiology, Department of Medicine, Indiana University School of Medicine, Indianapolis, IN, USA

Mailing address: Boyoung Joung, MD, PhD, Yonsei University College of Medicine, 250 Seungsanno, Seodaemun-gu, Seoul 120-752, Republic of Korea. E-mail: cby6908@yuhs.ac

ISSN-1346-9843 doi:10.1253/circj.CJ-12-1615

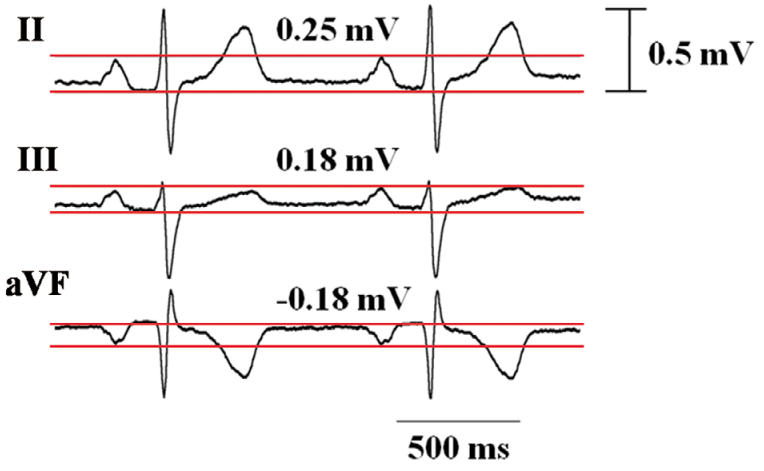

Figure 1. The height or depth of the P wave was measured from the peak or nadir, respectively, to the isoelectric line (TP interval).

Methods

Study Population

This prospective research study was approved by the Clinical Research and Ethics Committee of the Yonsei University Hospital, Seoul, South Korea, where all mapping studies were performed. Written informed consent was given by each patient. We excluded patients from the study if they had a recent (≤3 months) myocardial infarction, ongoing myocardial ischemia, heart failure, valvular heart diseases or sick sinus syndrome (SSS) prior to amiodarone treatment.

In a matched-cohort design, 18 patients (amiodarone group) who had undergone AF ablation while taking amiodarone were matched for age, sex and type of AF with 18 patients who had undergone AF ablation without taking amiodarone (no-amiodarone group). The patients in the no-amiodarone group were selected from 171 patients who were referred for electrophysiological study for ablation of symptomatic AF without taking amiodarone. We also excluded patients with SSS before the use of antiarrhythmic medication from both groups. SSS was defined as a syndrome encompassing a number of sinus nodal abnormalities, including sinus bradycardia, sinus arrest or block, SA conduction disturbance, and bradycardia-tachycardia syndrome.[14] We performed 3D endocardial mapping of the right atrium (RA) at baseline and during isoproterenol infusion in all patients. All antiarrhythmic medications (including β-blockers and calcium blockers) were suspended for > 5 half-lives before the study, excepting amiodarone.

Electrophysiological Study

Electrophysiological studies were performed in the postabsorptive state. The patients were sedated with midazolam and fentanyl. Multipolar catheters were positioned as follows: (1) 20-pole catheter with 2–5–2-mm interelectrode spacing in the coronary sinus with the proximal 10 electrodes positioned at the lateral RA; (2) 10-pole catheter with 2–7–2-mm interelectrode spacing along the lateral RA. Surface ECG and bipolar endocardial electrograms were monitored continuously and stored on a computer-based digital amplifier/recorder system with optical disk storage for offline analysis. Intracardiac electrograms were filtered from 30 to 500 Hz and measured with computer-assisted calipers at a sweep speed of 400 mm/s.

SAN function was evaluated as follows: (1) baseline sinus cycle length (CL) was determined over 10 consecutive sinus cycles; (2) SAN conduction time was determined after an 8-beat pacing train using the following formula: SAN conduction time=[return–basic cycle length]/2; the SAN conduction time was measured 3 times and the averaged value was used for data analyses; and (3) corrected SAN recovery time (CSNRT) was determined after a 30-s drive train at CL of 600 ms, correcting for the baseline CL. SAN conduction time and CSNRT was determined 3 times and the average value was used for analyses. CSNRT ≤550 ms was considered normal.[15]

Atrial effective refractory periods (ERPs) were evaluated with S_2 strength at twice the diastolic threshold current (for a pacing threshold <2 mA) after 8 S_1 paced beats at CLs of 600, 500, and 400 ms. An incremental technique was used, starting with an S_1–S_2 coupling interval of 150 ms. The coupling interval was then increased in 5-ms increments until S_2 captured the atria. The ERP was defined as the longest coupling interval that failed to capture the atria. ERP was measured 3 times each from the distal and proximal coronary sinus and from the low and high lateral RA. The averaged values were used for analyses.

Conduction velocity was assessed along the coronary sinus by pacing from the distal bipole (1–2) of the coronary sinus catheter and measuring the activation time at the proximal bipole (9–10), and along the lateral RA by pacing from the distal bipole (1–2) of the lateral RA catheter and measuring time to activate the proximal bipoles (9–10). At both sites, conduction was measured at pacing CLs of 600, 500, and 400 ms during stable capture. Conduction time was determined 10 times at each CL and the average value was used for analyses.

Surface 12-lead ECG P-wave morphology was assessed as previously described.[16] P waves were included for analysis only if an isoelectric interval was present and there was no fusion with the preceding QRS or T wave. P waves were described on the basis of the deviation from baseline during the TP interval as being: (1) positive (+); (2) negative (–); (3) isoelectric: arbitrarily defined when there was no P-wave deviation from a baseline of ≥0.05 mV; and (4) biphasic (+/– or –/+). The height or depth of the P wave was measured from the wave's peak or nadir to the isoelectric line (TP interval) using the electronic caliper of Pruka system (GE Healthcare, Milwaukee, WI, USA) (**Figure 1**).

Electroanatomic Mapping

The 3D mapping was recorded after circumferential pulmonary vein isolation and/or linear ablation in the left atrium (LA).

Table 1. Clinical Characteristics of the AF Patients With and Without Amiodarone Therapy

	No-amiodarone (n=18)	Amiodarone (n=18)	P value
Male	14 (78)	14 (78)	1.0
Age, years	62 (58–66)	61 (57–65)	0.89
Age >75 years	0	0	–
Type of AF, n (%)			1.0
PAF	8 (44)	8 (44)	
PeAF	10 (66)	10 (66)	
LA dimension, mm	41.4 (39.3–43.6)	43.7 (41.1–46.0)	0.19
LVEF, %	65.2 (63.1–67.2)	62.7 (59.2–66.2)	0.25
Underlying diseases			
Heart failure	0	0	–
Hypertension	8 (33)	9 (48)	1.0
Diabetes	0	3 (17)	0.23
Stroke	3 (18)	1 (6)	0.29
$CHADS_2$ score	0.8 (0.4–1.4)	0.8 (0.4–1.2)	0.87
P-wave duration, ms	96 (85–106)	111 (103–119)	0.03
P-wave amplitude, mV	0.12 (0.10–0.13)	0.13 (0.11–0.15)	0.35
Average 24-h heart rate, beats/min	63 (61–67)	77 (74–84)	0.004
Maximum RR interval, s	2,540 (1,755–3,270)	1,280 (1,080–1,945)	0.009
ERP, ms			
High RA	217 (205–231)	246 (235–258)	0.006
Low RA	212 (200–225)	245 (231–261)	0.004
Proximal CS	239 (226–252)	248 (237–259)	0.31
Distal CS	232 (213–254)	252 (238–269)	0.16
RA CV, m/s	0.60 (0.52–0.67)	0.53 (0.46–0.61)	0.23
LA CV, m/s	1.05 (0.96–1.14)	0.93 (0.80–1.06)	0.16

Data are n (%) or mean (95% CI). AF, atrial fibrillation; $CHADS_2$, congestive heart failure, hypertension, age ≥75 years, diabetes mellitus, and prior stroke or transient ischemic attack; CI, confidence interval; CS, coronary sinus; CV, conduction velocity; ERP, effective refractory period; LA, left atrium; LVEF, left ventricular ejection fraction; PAF, paroxysmal atrial fibrillation; PeAF, persistent atrial fibrillation.

Table 2. CSNRT and EAS at Baseline and During Isoproterenol Infusion in AF Patients With and Without Amiodarone Therapy

	No-amiodarone (n=18)	Amiodarone (n=18)	P value
SAN dysfunction, n (%)	0	4 (22)	0.03
No. patients with CSNRT >550 ms	0	5 (29)	0.02
CSNRT, ms	365 (232–449)	439 (391–693)	0.04
SANCT, ms	135 (114–156)	185 (152–219)	0.02
Baseline			
Heart rate, beats/min	80 (72–88)	66 (59–73)	0.01
EAS			0.37
Unicentric	14 (78)	16 (89)	
Multicentric	4 (22)	2 (11)	
EAS location, mm*	10.6 (3.4–15.1)	20.5 (10.8–25.5)	0.04
Isoproterenol			
Heart rate, beats/min	125 (118–131)	114 (108–120)	0.03
EAS, n (%)			0.55
Unicentric	16 (89)	17 (94)	
Multicentric	2 (11)	1 (6)	
EAS location, mm*	4.9 (1.6–8.4)	17.6 (7.7–29.0)	0.03

Data are n (%) or mean (95% CI), unless otherwise indicated. *EAS location is expressed by distance (mean and 25–75% range) from SVC-RA junction to the most cranial EAS. AF, atrial fibrillation; CI, confidence interval; CSNRT, corrected sinoatrial node recovery time; EAS, earliest activation site; RA, right atrium; SAN, sinoatrial node; SANCT, sinoatrial node conduction time; SVC, superior vena cava.

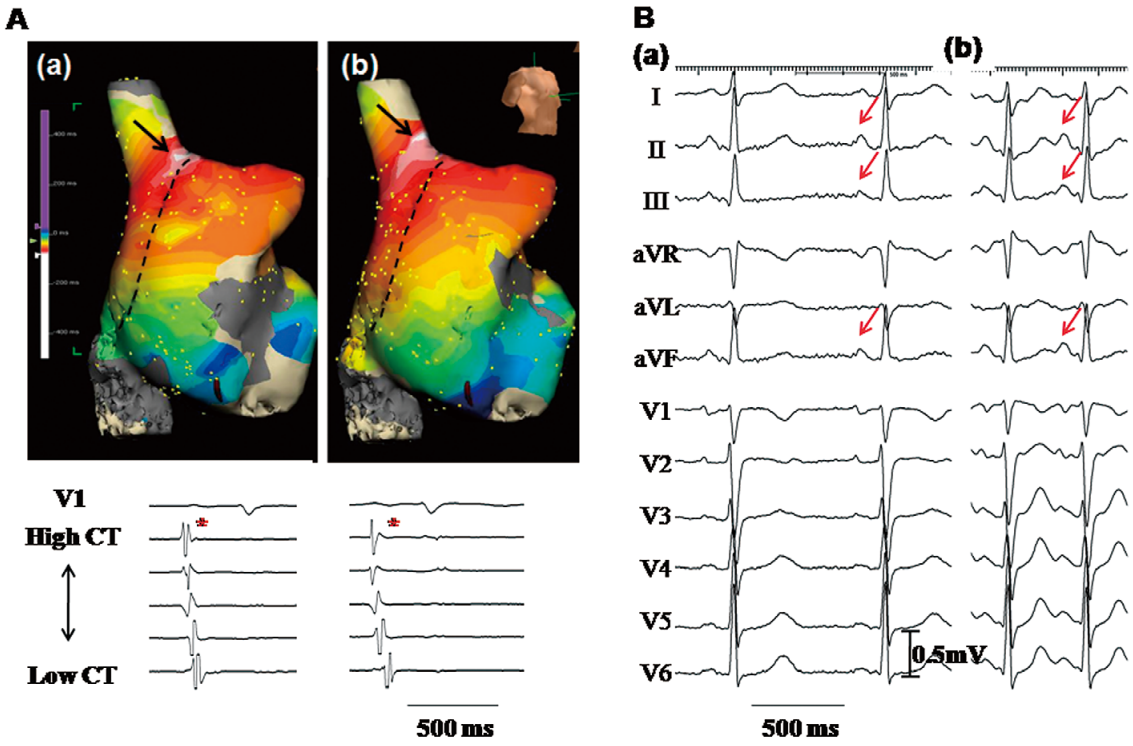

Figure 2. Effects of isoproterenol infusion on the earliest activation site (EAS) in a patient not taking amiodarone. (**A**) The right atrium (RA) activation maps (**Upper panels**) and electrograms (**Lower panels**). (**a**) The EAS at baseline, located at the junction between the superior vena cava (SVC) and RA (arrow). (**b**) The EAS during isoproterenol infusion, located at the SVC (arrow). *EAS of the crista terminalis. The dashed line in each panel marks the crista terminalis. (**B**) ECGs at baseline (**a**) and during isoproterenol infusion (**b**). There are tall positive P waves in leads II, III and aV_F (arrows) at baseline and during isoproterenol infusion.

Autonomic denervation was not performed. No ablation was performed in the RA or near the SAN. Electroanatomic maps of the RA were created before and during isoproterenol infusion using either the Ensite NavX (n=33 patients) or CARTO mapping system (n=3 patients). These systems record the 12-lead ECG and bipolar electrograms filtered at 30–200 Hz from the mapping catheter and the reference electrogram. Fluoroscopy, RA angiography and computerized tomography, and the Ensite NavX or CARTO merging were used to facilitate mapping of anatomic structures, particularly the crista terminalis and the junction of the superior vena cava (SVC) and the RA (SVC-RA), and for ensuring endocardial contact when individual points were acquired. High-density mapping was performed along the crista terminalis, septal RA, and areas of low voltage. Points were acquired if the stability criteria in space (≤6 mm) and local activation time (≤5 ms) were met.[17,18] Editing of points was performed offline. Local activation was manually annotated to the beginning of the first rapid deflection from the isoelectric line on bipolar electrograms. Points were excluded if they did not conform to the 12-lead ECG P-wave morphology or if they were <75% of the maximum voltage of the preceding electrogram. Bipolar voltage amplitudes were measure at high and low sites of the lateral, septal and posterior RA.

The linear distance from the SVC-RA junction to the most cranial EAS (earliest activation site) was used as a quantitative measure of EAS location.[13] To evaluate the SAN activation patterns, the following definitions were assigned: (1) unicentric: a single EAS that spread centrifugally to activate the atria, and (2) multicentric: ≥2 origins of impulses around the SAN with activation time difference ≤5 ms separated by a distance ≥10 mm.[19] The mapping was performed both at baseline and during isoproterenol infusion. The mapping during isoproterenol infusion of 10 μg/min was performed at the stable heart rate, approximately 5 min after the commencement of isoproterenol infusion.

Statistical Analysis

Continuous variables that are normally distributed are reported as mean±SD or 95% confidence interval (CI). Student's t-test was used to compare the means of continuous variables that are approximately normally distributed between the 2 groups. Continuous variables that were not normally distributed (the distance from the SVC-RA junction to the most cranial EAS, CSNRT and SAN conduction time) are reported as median (25–75 percentile range) and compared using Kruskal-Wallis test. Normality was determined using the Kolmogorov-Smirnov goodness-of-fit test. Categorical variables are reported as count (percentage) and compared using Fisher's exact test. An exact 95% CI was calculated for percentage estimates discussed in the text. The correlation between the distance from the SVC-RA junction to the most cranial EAS and P-wave amplitude was evaluated with Pearson correlation. The means of paired P-wave amplitudes (baseline and isoproterenol infusion) were evaluated with the paired t-test. The SPSS statistical package (SPSS Inc, Chicago, IL, USA) was used to perform all statistical evaluations. A P value of ≤0.05 was considered statistically

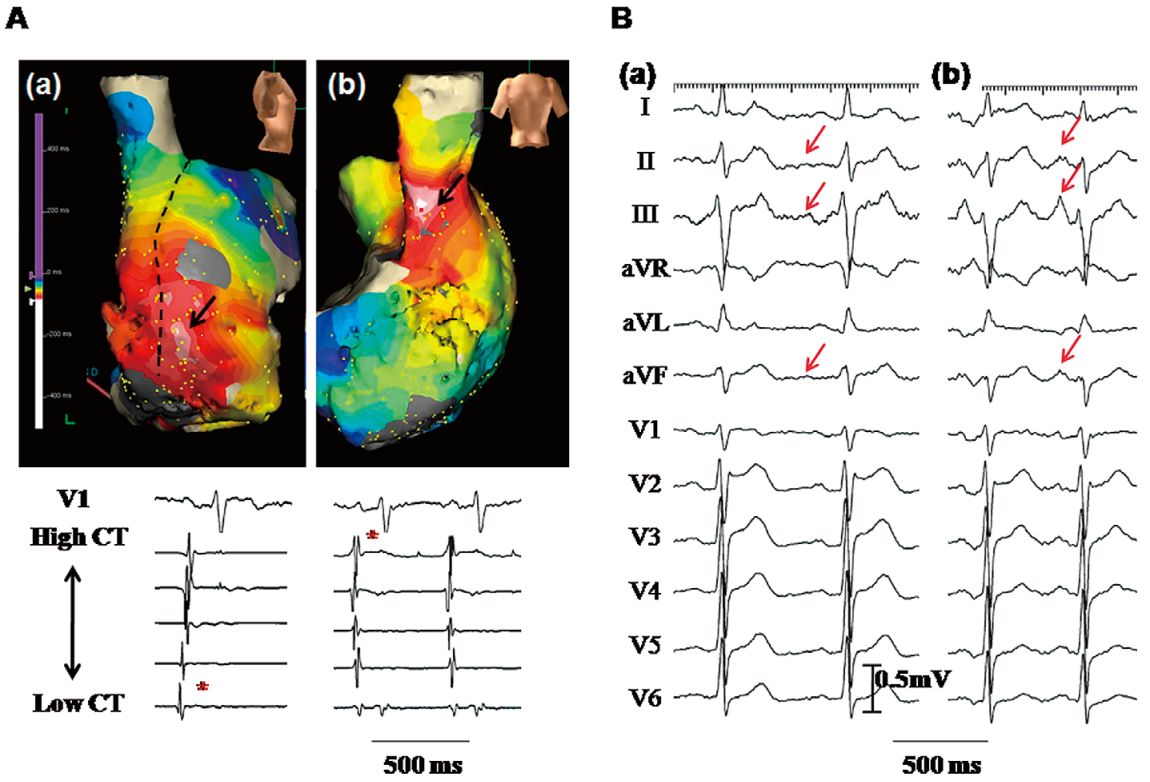

Figure 3. Superior shift of the earliest activation site (EAS) during isoproterenol infusion in a patient taking amiodarone. (**A**) The right atrium (RA) activation maps (**Upper panels**) and electrograms (**Lower panels**). (**a**) The EAS at baseline, located in the inferior part of crista terminalis (arrow). (**b**) The EAS during isoproterenol infusion, having shifted to the junction of the superior vena cava and RA (arrow). *EAS of the crista terminalis. The dashed line in each panel marks the crista terminalis. (**B**) ECGs at baseline (**a**) and during isoproterenol infusion (**b**). Note the increased amplitude of the P waves in leads II, III and aV_F after superior shift of the EAS during isoproterenol infusion (arrows).

significant.

Results

Patients' Characteristics

The comparison of the baseline characteristics of the 2 groups is presented in Table 1. The amiodarone group included 14 (78%) males with a mean age of 61 (57–65) years. The no-amiodarone group included 14 (78%) males with a mean age of 62 (58–66) years. There were no differences between the 2 groups in LA dimensions, underlying diseases and $CHADS_2$ score. At the discretion of the patients' doctors, the antiarrhythmic medications were prescribed, and the mean number was 1.5 (1.2–1.7) and 1.2 (1.1–1.4), respectively, in the amiodarone and no-amiodarone groups (P=0.17). Class Ic drugs (flecainide, n=17; pilsicainide, n=1) and a class III drug (sotalol, n=4) were used as the first and second antiarrhythmic drugs, respectively, in the no-amiodarone group. In the amiodarone group, amiodarone (n=8), flecainide (n=5), pilsicainide (n=2) and sotalol (n=1) were used as the first-choice antiarrhythmic drug. The mean duration and cumulative dosage of amiodarone were 145 (89–221) days and 28,989 (17,667–43,739) mg, respectively. Daily maintenance dosage of amiodarone was 200 mg in the amiodarone group. Thyroid function was within normal range in all 4 patients with sinus node disease. The amiodarone group (111, 103–119 ms) had significantly longer P-wave duration than the no-amiodarone group (96, 85–106 ms, P=0.03). P-wave amplitude did not differ between groups.

SAN Dysfunction and Amiodarone

No patient in either group showed clinical evidence of SAN dysfunction before antiarrhythmic medications. However, after antiarrhythmic treatment, Holter monitoring showed a lower average 24-h heart rate and longer maximum RR interval in the amiodarone group compared with the no-amiodarone group (Table 1). After amiodarone medication, 4 (22%) patients (Table 2) developed SSS that warranted pacemaker implantation; 1 of the 4 patients had inappropriate sinus bradycardia and 3 had pauses at the termination of AF, causing dizziness or syncope. Abnormal CSNRT (>550 ms) was found in 3 of these 4 patients and another 2 patients without symptomatic bradycardia. No patients in the control group showed SSS or abnormal CSNRT. The median value of CSNRT and SAN conduction time were significantly longer in the amiodarone group than in the controls at a pacing CL of 500 ms.

SAN Response to Sympathetic Stimulation

Baseline heart rate was 80 (72–88) beats/min in the no-amiodarone group, and 66 (59–73) beats/min in the amiodarone group. The mean maximum heart rate during isoproterenol infusion was 125 (118–131) beats/min and 114 (108–120) beats/min, respectively. The amiodarone group had a significantly lower

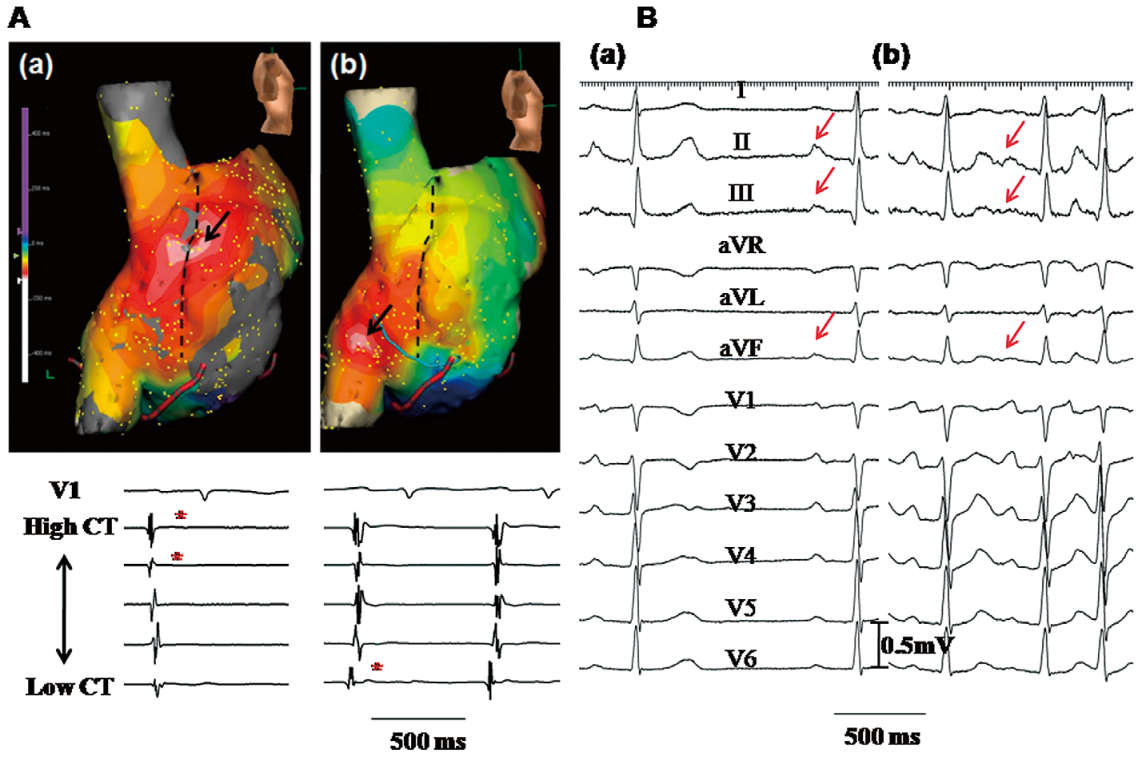

Figure 4. Inferior shift of the earliest activation site (EAS) during isoproterenol infusion in a patient taking amiodarone. (**A**) The right atrium (RA) activation maps (**Upper panels**) and electrograms (**Lower panels**). (**a**) The EAS at baseline, located in the mid-portion of the crista terminalis (arrow). (**b**) The EAS during isoproterenol infusion, having shifted to the lower part of the crista terminalis (arrow). *EAS of the crista terminalis. The dashed line in each panel marks the crista terminalis. (**B**) ECGs at baseline (**a**) and during isoproterenol infusion (**b**). Note the decreased amplitude of the P waves in leada II, III and aV_F after inferior shift of EAS during isoproterenol infusion (arrows).

heart rate than the no-amiodarone group at baseline (P=0.01) and during isoproterenol infusion (P=0.03, **Table 2**).

Using 3D mapping, we analyzed a mean of 237±30 and 210±25 points per patient during sinus rhythm and isoproterenol infusion, respectively. There were no significant differences between groups in the number of points analyzed at baseline (P=0.29) and during isoproterenol infusion (P=0.14). **Figure 2A-a** shows a unicentric EAS (arrow) at baseline within the SVC-RA junction. The EAS moved to the SVC during isoproterenol infusion (arrow in **Figure 2A-b**). The P-wave morphology at baseline and during isoproterenol infusion did not differ (**Figure 2B**).

Figure 3 shows superior shift of EAS during isoproterenol infusion in a patient taking amiodarone. The EAS was located at the inferior part of crista terminalis (**Figure 3A-a**) and associated with an isoelectric or inverted (negative) P-wave in the inferior leads (II, III and aV_F) (**Figure 3B-a**). Isoproterenol administration shifted the EAS to the SVC-RA junction (**Figure 3A-b**), together with a normalization of P-wave morphology (**Figure 3B-b**). **Figure 4** shows a typical example of unresponsiveness of the SAN to isoproterenol infusion in an AF patient taking amiodarone. The EAS at baseline was located at the mid-portion of the crista terminalis (arrow in **Figure 4A-a**) with upright, low-amplitude P waves (**Figure 4B-a**). During 10 μg/min isoproterenol infusion, the EAS moved to the inferior vena cava-RA junction (arrow in **Figure 4A-b**), together with a reduction in P-wave amplitudes in the inferior leads (**Figure 4B-b**). The superior part of the SAN in this patient was always activated passively with and without isoproterenol infusion. For all patients studied, the downward shift of the EAS during isoproterenol infusion was observed in 2 (11%) of 18 patients in the no-amiodarone group and in 6 (33%) of 18 patients in the amiodarone group (P=0.11).

Figure 5 summarizes the unicentric EAS in the no-amiodarone and amiodarone patients at baseline (**Figure 5A**) and during isoproterenol infusion (**Figure 5B**). The median distance from the SVC-RA junction to the most cranial EAS was 10.6 (3.4–15.1) mm for the no-amiodarone and 20.5 (10.8–25.5) mm for the amiodarone group at baseline (**Table 2**, **Figure 5C**). The EAS was located significantly more superior (cranial) in the no-amiodarone than in the amiodarone group (P=0.04). During isoproterenol infusion, the distance from the SVC-RA junction to the most cranial EAS significantly shortened to 5.6 (0.4–10.8) mm in the no-amiodarone group (P=0.04), but insignificantly to 4.0 (–4.3–12.0) mm in the amiodarone group (P=0.37). The median distance from the SVC–RA junction to the most cranial EAS was 4.9 (1.6–8.4) mm in the no-amiodarone group and 17.6 (7.7–29.0) mm in the amiodarone group during isoproterenol infusion (**Figure 5C**). The distance from the SVC to the most cranial EAS was longer in the amiodarone than in the no-amiodarone group during isoproterenol infusion (P=0.03). Multicentric activation patterns did not differ between the 2 groups at baseline (P=0.37) or during isoproterenol infusion (**Table 2**, P=0.55).

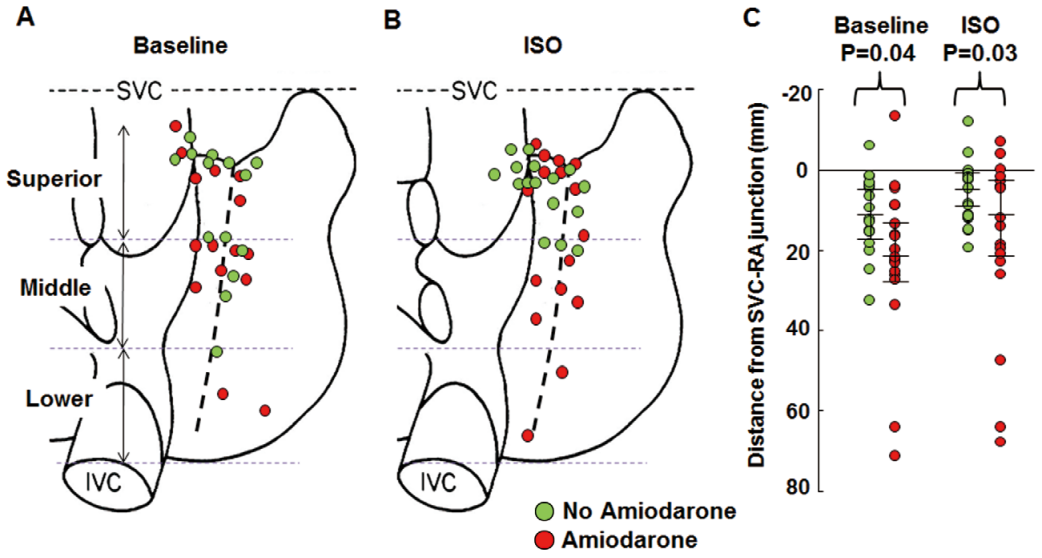

Figure 5. Distribution of the unicentric earliest activation site (EAS) at baseline (**A**) and during isoproterenol (ISO) infusion (**B**). Green and red circles represent the no-amiodarone and amiodarone groups, respectively. (**C**) The distance from the SVC-RA junction to the most cranial EAS at baseline and during isoproterenol infusion. IVC, inferior vena cava; RA, right atrium; SVC, superior vena cava.

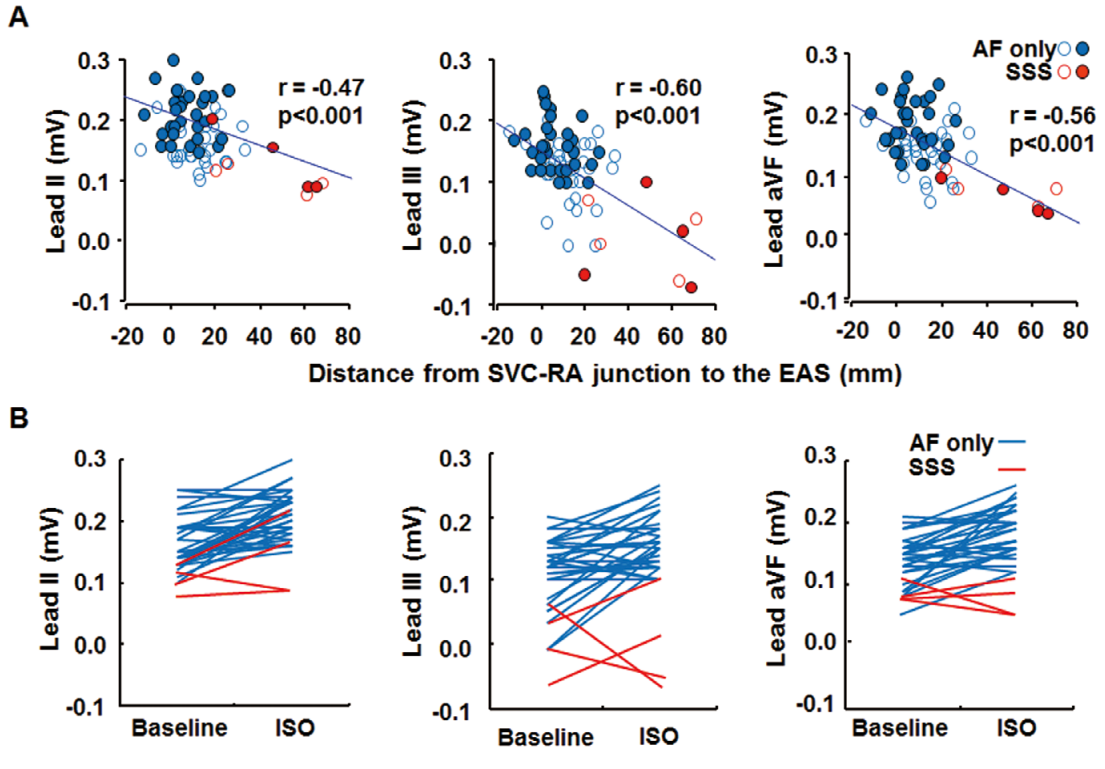

Figure 6. Change in the P wave by sympathetic stimulation. (**A**) Negative correlation between the distance from the SVC-RA junction to the most cranial EAS and P-wave amplitude in leads II (**Left**), III (**Middle**) and aV$_F$ (**Right**). Unfilled and filled circles represent P-wave amplitude at baseline and during isoproterenol (ISO) infusion, respectively. Red and blue circles represent the patient with and without sick sinus syndrome (SSS), respectively. (**B**) Change in P-wave amplitude in leads II (**Left**), III (**Middle**) and aV$_F$ (**Right**) during ISO infusion. Note that the patients with SSS tend to have low P-wave amplitude and low EAS location at both baseline and during ISO infusion.

P-Wave Morphology and the Distance From the SVC-RA Junction to the EAS

The distance from the SVC-RA junction to the most cranial EAS negatively correlated with the P-wave amplitudes of leads II (r=–0.47, P<0.001), III (r=–0.60, P<0.001) and aV_F (r=–0.56, P<0.001, **Figure 6A**: the P-wave amplitudes of the 4 patients with SSS were marked in red).

Figure 6B shows the change in P-wave amplitude during isoproterenol infusion in patients with and without SSS. P-wave amplitudes in leads II (0.17±0.04 vs. 0.21±0.04 mV, P<0.001), III (0.12±0.05 vs. 0.16±0.04 mV, P<0.001) and aV_F (0.14±0.04 vs. 0.19±0.04 mV, P<0.001) were increased significantly in patients without SSS. In comparison, P-wave amplitudes in leads II (0.11±0.02, vs. 0.14±0.06 mV, P=0.33), III (0.01±0.06, vs. 0.0±0.08 mV, P=0.82) and aV_F (0.08±0.02, vs. 0.07±0.03 mV, P=0.57) were not increased in patients with SSS.

Other Electrophysiological Characteristics of the Amiodarone Group

The ERP and conduction velocity of the 2 groups are detailed in **Table 1**. ERPs of the high RA were 246 (235–258) ms and 217 (205–231) ms for the amiodarone and no-amiodarone group, respectively. The ERPs of the high (P=0.006) and low RA (P=0.004) were longer in the amiodarone than in the no-amiodarone group. However, ERPs measured at the proximal and distal coronary sinus showed no difference between groups. There was no difference in the RA conduction velocity along the RA catheter and LA conduction velocity along the coronary sinus catheter between groups either.

Discussion

Major Findings

SAN dysfunction was observed in one-quarter of the AF patients receiving amiodarone. The EAS was located more caudally in the amiodarone than in the no-amiodarone group at baseline and during isoproterenol infusion, suggesting that dysfunction and unresponsiveness of the superior SAN to sympathetic stimulation might be a mechanism of SAN dysfunction during amiodarone therapy. We also found that the P-wave morphology may be used to assess the EAS location during isoproterenol infusion. Analyses of P-wave morphology before and after isoproterenol infusion may be helpful in determining the function of the SAN.

Amiodarone and SAN Dysfunction

Amiodarone is an iodinated benzofuran derivative that blocks multiple channels (I_{to}, I_{Kr}, I_{Ks}, I_{Ca}, I_{Na}), and also has β-adrenergic blocking effects.[12] Amiodarone impaired SAN function in one-third of patients and was associated with an increased risk of pacemaker insertion.[5] In the present study, amiodarone induced SAN dysfunction in one-quarter of patients without SAN dysfunction at baseline. A variety of studies has shown that procainamide, quinidine, lidocaine, mexiletine, propafenone and sotalol can adversely affect SAN function in patients with evidence of SAN dysfunction.[15] However, we did not observe clinically significant SAN dysfunction in patients in the no-amiodarone group. These other antiarrhythmic agents may not have as profound an effect on the calcium clock as amiodarone, which is a potent blocker of the I_{Ca}.[12] The latter effects may suppress the Ca^{2+} clock in the SAN.[20] In addition, amiodarone can inhibit sympathetic activity. A downward shift of the EAS has been reported in human patients after esmolol infusion.[21] Therefore, the β blocking effects of amiodarone may also influence the location of the EAS. Finally, amiodarone may induce hypothyroidism, and this effect may, in part, affect the Ca^{2+} clock.

Amiodarone and Impaired Heart Rate Acceleration to Sympathetic Stimulation

Schuessler et al reported that sympathetic stimulation in a canine model in general tended to induce a cranial shift in the location of the pacemaker within the pacemaker complex.[22] The unresponsiveness of the superior SAN to sympathetic stimulation is a characteristic finding of SAN dysfunction.[10,13] In the present study, amiodarone administration was associated with impaired heart rate acceleration and impaired cranial shift of the EAS after sympathetic stimulation. Our group previously reported that during β-adrenergic stimulation in a canine model of intact SAN, heart rate accelerated with a cranial shift of the pacemaking site and late diastolic Ca^{2+} elevation, which is closely related with spontaneous SR Ca^{2+} release.[8] Therefore, the Ca^{2+} clock malfunction of the superior SAN might be related to impaired heart rate acceleration and a cranial shift in the pacemaking site.

P-Wave Morphology and the EAS

Atrial tachycardias originating from the crista terminalis can be differentiated by their P-wave morphology. A P-wave morphology that includes positive polarity in leads I and II, negative in aV_R, and biphasic (positive-negative) in V_1 (and, if positive in V_1 in tachycardia, then also positive in sinus rhythm) is associated with a foci at the crista terminalis.[23] In the present study, we found that the distance from the SVC-RA junction to the EAS negatively correlated with the amplitude of the P waves in leads II, III and aV_F. If the EAS shifted to the superior part of the crista terminalis or SVC, the P-wave amplitudes increased in most of the patients without SAN dysfunction. In contrast, a shift of the EAS to the inferior part of the crista terminalis or inferior vena cava was related to decreased P-wave amplitude in leads II, III, and aV_F in patients with SAN dysfunction. These findings suggest that the P-wave morphology during isoproterenol infusion may be used to assess the superior SAN's responsiveness to isoproterenol infusion. Inverted or isoelectric P waves at baseline that fail to normalize during isoproterenol infusion suggest abnormal SAN function.

Study Limitations

This was not a prospective randomized trial. To evaluate the effect of amiodarone, a comparison of sinus node function before and after treatment with amiodarone in the same patients with AF is required. However, performing such invasive tests twice in a clinical setting is difficult. Thus, we chose a case-control design for this study. There might be potential confounders that were not eliminated by the matched-cohort design. The amiodarone group might be different and sicker from the start than the no-amiodarone group. However, because we excluded patients with SSS from enrollment in either group, the possibility that the amiodarone group included patients with SSS is very low. Because all patients had AF, it is possible that all patients had some degree of sinus node dysfunction. However, the development of SSS on amiodarone therapy in 22% of the patients, but in none of the control group of patients, suggests that amiodarone has significant differential effects on sinus node dysfunction.

Conclusions

SAN dysfunction was observed in one-quarter of AF patients

receiving amiodarone. Amiodarone induced SAN dysfunction in one-quarter of patients with AF. The EAS was located more caudally in the amiodarone group than in the no-amiodarone group at baseline and during isoproterenol infusion, suggesting that unresponsiveness of the superior SAN to sympathetic stimulation could be a mechanism of the SAN dysfunction induced by amiodarone. These findings suggest that Ca^{2+} clock malfunction might be 1 of the mechanisms underlying sinus node dysfunction.

Acknowledgments

We thank Chung-Ki Lee and Hyun-Jae Park for their technical support.

Disclosures

No conflict of interest.

Author Contributions

The authors had full access to and take full responsibility for the integrity of the data. All authors read and agreed to the manuscript as written.

Dr Mun acquired, analyzed, interpreted the data, and drafted the manuscript. Dr Pak, Dr Lee, and Dr Lin assisted the data analysis and interpretation. PhD student Shen assisted with the statistical analysis. Dr Chen and Dr Joung conceived and designed the research, and handled the funding as well as the supervision. All co-authors have read and approved the submission of this manuscript.

Names of Grants

This study was supported in part by research grants of the Basic Science Research Program through the National Research Foundation of Korea, funded by the Ministry of Education, Science and Technology (2012-0007604, 2012-045367), a grant of the Korean Healthcare technology R&D project, funded by Ministry of Health & Welfare (A121668), and by United States NIH grants P01 HL78931, R01 HL78932, R01 HL71140, the Krannert Endowment, the Medtronic-Zipes Endowment and the Strategic Research Initiative of the Indiana University Health and the Indiana University School of Medicine.

References

1. Aronow WS. Management of the older person with atrial fibrillation. *J Am Geriatr Soc* 1999; **47:** 740–748.
2. Chugh SS, Blackshear JL, Shen WK, Hammill SC, Gersh BJ. Epidemiology and natural history of atrial fibrillation: Clinical implications. *J Am Coll Cardiol* 2001; **37:** 371–378.
3. Go AS, Hylek EM, Phillips KA, Chang Y, Henault LE, Selby JV, et al. Prevalence of diagnosed atrial fibrillation in adults: National implications for rhythm management and stroke prevention: The AnticoagulationandRisk factors in Atrial Fibrillation (ATRIA) study. *JAMA* 2001; **285:** 2370–2375.
4. Moon J, Hong YJ, Shim J, Hwang HJ, Kim JY, Pak HN, et al. Right atrial anatomical remodeling affects early outcomes of nonvalvular atrial fibrillation after radiofrequency ablation. *Circ J* 2012; **76:** 860–867.
5. Essebag V, Hadjis T, Platt RW, Pilote L. Amiodarone and the risk of bradyarrhythmia requiring permanent pacemaker in elderly patients with atrial fibrillation and prior myocardial infarction. *J Am Coll Cardiol* 2003; **41:** 249–254.
6. DiFrancesco D. The role of the funny current in pacemaker activity. *Circ Res* 2010; **106:** 434–446.
7. Lakatta EG, Maltsev VA, Vinogradova TM. A coupled system of intracellular Ca^{2+} clocks and surface membrane voltage clocks controls the timekeeping mechanism of the heart's pacemaker. *Circ Res* 2010; **106:** 659–673.
8. Joung B, Tang L, Maruyama M, Han S, Chen Z, Stucky M, et al. Intracellular calcium dynamics and acceleration of sinus rhythm by beta-adrenergic stimulation. *Circulation* 2009; **119:** 788–796.
9. Shinohara T, Park HW, Joung B, Maruyama M, Chua SK, Han S, et al. Selective sinoatrial node optical mapping and the mechanism of sinus rate acceleration. *Circ J* 2012; **76:** 309–316.
10. Joung B, Lin SF, Chen Z, Antoun PS, Maruyama M, Han S, et al. Mechanisms of sinoatrial node dysfunction in a canine model of pacing-induced atrial fibrillation. *Heart Rhythm* 2010; **7:** 88–95.
11. Joung B, Shinohara T, Zhang H, Kim D, Choi EK, On YK, et al. Tachybradycardia in the isolated canine right atrium induced by chronic sympathetic stimulation and pacemaker current inhibition. *Am J Physiol Heart Circ Physiol* 2010; **299:** H634–H642.
12. Kodama I, Kamiya K, Toyama J. Cellular electropharmacology of amiodarone. *Cardiovasc Res* 1997; **35:** 13–29.
13. Joung B, Hwang HJ, Pak HN, Lee MH, Shen C, Lin SF, et al. Abnormal response of superior sinoatrial node to sympathetic stimulation is a characteristic finding in patients with atrial fibrillation and symptomatic bradycardia. *Circ Arrhythm Electrophysiol* 2011; **4:** 799–807.
14. Zipes DP. Cardiac electrophysiology: From cell to bedside. Saunders, New York, 2009.
15. Josephson ME. Clinical cardiac electrophysiology: Techniques and interpretations. Lippincott Williams & Wilkins, Philadelphia, 2008.
16. Tang CW, Scheinman MM, Van Hare GF, Epstein LM, Fitzpatrick AP, Lee RJ, et al. Use of p wave configuration during atrial tachycardia to predict site of origin. *J Am Coll Cardiol* 1995; **26:** 1315–1324.
17. Sanders P, Kistler PM, Morton JB, Spence SJ, Kalman JM. Remodeling of sinus node function in patients with congestive heart failure: Reduction in sinus node reserve. *Circulation* 2004; **110:** 897–903.
18. Sanders P, Morton JB, Kistler PM, Spence SJ, Davidson NC, Hussin A, et al. Electrophysiological and electroanatomic characterization of the atria in sinus node disease: Evidence of diffuse atrial remodeling. *Circulation* 2004; **109:** 1514–1522.
19. Boineau JP, Canavan TE, Schuessler RB, Cain ME, Corr PB, Cox JL. Demonstration of a widely distributed atrial pacemaker complex in the human heart. *Circulation* 1988; **77:** 1221–1237.
20. Maltsev VA, Lakatta EG. Dynamic interactions of an intracellular Ca^{2+} clock and membrane ion channel clock underlie robust initiation and regulation of cardiac pacemaker function. *Cardiovasc Res* 2008; **77:** 274–284.
21. Marrouche NF, Beheiry S, Tomassoni G, Cole C, Bash D, Dresing T, et al. Three-dimensional nonfluoroscopic mapping and ablation of inappropriate sinus tachycardia: Procedural strategies and long-term outcome. *J Am Coll Cardiol* 2002; **39:** 1046–1054.
22. Schuessler RB, Boineau JP, Wylds AC, Hill DA, Miller CB, Roeske WR. Effect of canine cardiac nerves on heart rate, rhythm, and pacemaker location. *Am J Physiol* 1986; **250:** H630–H644.
23. Kistler PM, Roberts-Thomson KC, Haqqani HM, Fynn SP, Singarayar S, Vohra JK, et al. P-wave morphology in focal atrial tachycardia: Development of an algorithm to predict the anatomic site of origin. *J Am Coll Cardiol* 2006; **48:** 1010–1017.